HHS Public Access

Author manuscript

Acta Neuropathol. Author manuscript; available in PMC 2017 December 01.

Published in final edited form as:

Acta Neuropathol. 2016 December ; 132(6): 859–873. doi:10.1007/s00401-016-1637-y.

Depletion of TDP-43 decreases fibril and plaque β-amyloid and exacerbates neurodegeneration in an Alzheimer's mouse model

Katherine D. LaClair[1,3], **Aneesh Donde**[1,2], **Jonathan P. Ling**[1], **Yun Ha Jeong**[1,4], **Resham Chhabra**[1], **Lee J. Martin**[1,2], and **Philip C. Wong**[1,2,3]

[1] Department of Pathology, Johns Hopkins University School of Medicine, 720 Rutland Avenue, Ross 558, Baltimore, MD 21205, USA

[2] Department of Neuroscience, Johns Hopkins University School of Medicine, Baltimore, MD 21205, USA

[3] Cellular and Molecular Medicine Program, Johns Hopkins University School of Medicine, Baltimore, MD 21205, USA

Abstract

TDP-43 proteinopathy, initially associated with ALS and FTD, is also found in 30–60% of Alzheimer's disease (AD) cases and correlates with worsened cognition and neurodegeneration. A major component of this proteinopathy is depletion of this RNA-binding protein from the nucleus, which compromises repression of non-conserved cryptic exons in neurodegenerative diseases. To test whether nuclear depletion of TDP-43 may contribute to the pathogenesis of AD cases with TDP-43 proteinopathy, we examined the impact of depletion of TDP-43 in populations of neurons vulnerable in AD, and on neurodegeneration in an AD-linked context. Here, we show that some populations of pyramidal neurons that are selectively vulnerable in AD are also vulnerable to TDP-43 depletion in mice, while other forebrain neurons appear spared. Moreover, TDP-43 depletion in forebrain neurons of an AD mouse model exacerbates neurodegeneration, and correlates with increased prefibrillar oligomeric Aβ and decreased Aβ plaque burden. These findings support a role for nuclear depletion of TDP-43 in the pathogenesis of AD and provide strong rationale for developing novel therapeutics to alleviate the depletion of TDP-43 and functional antemortem biomarkers associated with its nuclear loss.

Keywords

TDP-43; Alzheimer's disease; β-Amyloid; Nuclear depletion; Forebrain

Philip C. Wong wong@jhmi.edu.

[4]Present Address: Neural Development and Disease Department, Korea Brain Research Institute, Daegu 701-300, Korea

Compliances with ethical standards

Conflict of interest The authors declare no competing financial interests.

Research involving animals or human participants All animal studies were performed in accordance with institutional guidelines and the laws of the United States of America. No research involved human participants in this study.

Introduction

Alzheimer's disease (AD) is the most common age-related dementia and the fifth most prevalent cause of death in the United States [2]. AD is associated with progressive loss of synapses, and eventually neurons, beginning in the hippocampus and frontal cortex [43, 52, 62]. While strong evidence supports an essentially linear progression of disease triggered by Aβ in familial AD, the evidence in sporadic AD cases supports a more multifactorial etiology [17, 40, 41]. First, the risk genes associated with sporadic AD are involved in diverse functions [18], and there is evidence that many have roles in neurodegeneration independent of Aβ [20, 31, 63]. Several of these AD risk genes are also implicated in neurodegenerative diseases with no Aβ pathology [20, 25]. Second, 20–40% of cognitively normal individuals have levels of Aβ and tau pathology that are indistinguishable from cases with severe clinical symptoms of AD [5, 11]. Together, these data suggest that non-canonical mechanisms other than Aβ and tau also contribute to neurodegeneration and cognitive failure in AD.

Interestingly, recent work showed that non-canonical pathologies occur in up to 75% of AD cases [33, 49], including TDP-43 proteinopathy, α-synuclein “Lewy bodies”, and tau “Pick bodies” that are associated with neurodegeneration in separately classified diseases [44, 48, 60]. TDP-43 proteinopathy is characterized by cytoplasmic aggregation of the transactivation response element DNA-binding protein 43 (TDP-43) accompanied by its nuclear clearance, and was first identified in another neurodegenerative disease spectrum, ALS-FTD [44]. Notably, TDP-43 proteinopathy is one of the most common non-canonical pathologies observed in AD cases [3] and is strongly associated with worsened neurodegeneration and cognition [27]. Previously, we found that TDP-43 is a splicing repressor of non-conserved cryptic exons and that this function is compromised in ALS-FTD [36]. Specifically, depletion of TDP-43 leads to incorporation of non-conserved cryptic exons that usually induce nonsense mediated decay of the associated mRNAs, thereby altering the proteome of affected cells.

The importance of disease mechanisms related to nuclear depletion of TDP-43 is underscored by independent studies showing that reducing the aggregation of cytoplasmic TDP-43 does not prevent its cytotoxicity [37], while simultaneously reintroducing TDP-43 to its nuclear location successfully reverses motor neuron deficits [65]. Importantly, our group recently found that TDP-43-associated cryptic exons are also incorporated in brains of AD cases with TDP-43 pathology (Chen et al., in review) suggesting that depletion of TDP-43 from neurons also contributes to the pathogenesis of AD. If so, neuron populations vulnerable in AD should also be selectively vulnerable to depletion of TDP-43, and depletion of TDP-43 should exacerbate neurodegeneration in an AD-linked mammalian context. To investigate these questions, we employed the tamoxifeninducible Cre^{ER} recombinase system to conditionally ablate *Tdp-43* in forebrain neurons of mature wild-type and $APP_{swe}/PS1\Delta E9$ mice, bypassing embryonic lethality caused by developmental loss of TDP-43 in the brain [9].

In these studies, we draw a distinction between neurodegeneration and neuron loss that we believe is important for accurate assessment of neurodegenerative processes in mouse

models. Neurodegeneration and the molecular processes that drive it may be exacerbated in the absence of frank neuron loss on relatively short time scales such as the life span of the mouse. For example, though *APP_{swe}/PS1ΔE9* mice notoriously do not show neuron loss, they exhibit significant synaptic and mitochondrial neurodegeneration [12, 68] and these pathological features are well suited to assess exacerbated neurodegeneration in an AD context. Here, we show for the first time that TDP-43 depletion in the forebrain selectively affects populations of pyramidal neurons that are vulnerable in AD, and exacerbates molecular and morphological neurodegeneration in *APP_{swe}/PS1ΔE9* mice. Interestingly, Aβ plaque burden is reduced in *APP/PS1* mice lacking TDP-43, and decreased levels of presynaptic proteins are instead strongly correlated with prefibril Aβ oligomers. Since depletion of TDP-43 may occur frequently in AD and other neurodegenerative diseases, these findings provide strong rationale to stratify clinical trials of Aβ-directed therapeutics by TDP-43 status, and underscore a need for functional antemortem biomarkers related to nuclear depletion of TDP-43.

Materials and methods

Mouse model

All mouse experiments complied with regulations of the Animal Care and Use Committee at Johns Hopkins University School of Medicine in accordance with the laws of the State of Maryland and the United States of America. We depleted TDP-43 in the forebrains of adult mice by generating *CaMKIIα-Cre^{ER};$Tdp\text{-}43^{F/F}$* (cT) mice with *loxP* sites flanking *Tdp-43* exon 3, allowing tamoxifen-induced recombination in excitatory forebrain neurons at maturity (Fig. 1a). Mature forebrain depletion of TDP-43 is consistent with the late onset of AD and regional specificity of neurodegeneration and TDP-43 proteinopathy in patients [4, 21, 28]. It is also necessary for these studies, because constitutive knockout of *Tdp-43* is embryonically lethal, and heterozygous knockout does not reduce the levels of TDP-43 protein [9]. *CaMKIIα*-Cre^{ER};$Tdp\text{-}43^{F/F}$ (cT) mice were generated and bred with the *APP_{swe}/PS1ΔE9* (AP) line (purchased from Jackson Labs) to generate a cohort of *CaMKIIα*-Cre^{ER};$Tdp\text{-}43^{F/F}$;*APP_{swe}/PS1ΔE9* (cTAP) mice on a C57BL/6J background, as well as littermate controls (Fig. 1b). In analysis of cT mice, we used equal numbers of male and female mice (Figs. 1, 2), or females only. For all experiments in Figs. 1 and 2, there were no differences between males and females, and the results are reported without reference to sex. For experiments in cTAP mice (Figs. 3, 4), we used females exclusively because of established phenotypic sex differences in the AP mouse model [6, 35].

Animals were genotyped at weaning, and mice were subsequently housed with one littermate of each genotype (4 mice/cage) when possible. Oral tamoxifen citrate was administered to all animals in the feed (Harlan Teklad) at an average 40 mg/kg/day for a 4-week period beginning at p42-46, and mice were singly housed during this period to monitor tamoxifen-feed intake. Afterwards, mice were returned to their original cage grouping with their littermates. No other tests, drug administration, or surgery were performed on these animals.

Studies were conducted in brain tissue from mice aged 3 to 14 months, collected from >10 L over 15 months. At designated ages, mice were deeply anesthetized using 200 μL/25 g of

15% chloral hydrate, then perfused briefly with ice cold PBS. The brains were removed, and one hemisphere was post-fixed in 4% paraformaldehyde for 24 h, while the other hemisphere was dissected into regions (cortex, hippocampus, cerebellum) and individually stored at −80 °C. For electron microscopy, one animal of each genotype was perfused with 4% paraformaldehyde following PBS perfusion. The brains were removed and placed in 4% paraformaldehyde +2% glutaraldehyde for 18 h. A <3 mm^3 region containing the CA1 was then dissected out and processed for electron microscopy using standard procedures by the Johns Hopkins School of Medicine Microscope Facility Core.

Immunoblot and ELISA

Hippocampal tissue was homogenized in 10 volumes of ice cold RIPA buffer supplemented with 1× Protease inhibitor cocktail (Roche) and 1× phosphatase inhibitor (PhosSTOP), then centrifuged at 12,000×*g* for 20 min at 4 °C. Alternatively, for ELISA, hippocampal tissue was homogenized in 8 volumes of 5-M Guanidine HCl, then processed for ELISA using the Thermo Fisher human Aβ 42 kit (KHB3441) according to the manufacturer's instructions. Protein levels in the supernatant were determined using the BCA assay, and 15 μg of protein was loaded onto 4–12% or 10% Bis–Tris gels (Novex) along with 10 μL SeeBlue Plus 2 pre-stained protein standard (Thermo Fisher), and transferred to PVDF membrane. Membranes were probed with antibodies to synaptophysin (1:15,000, Abcam SY38/ab8049], PSD-95 (1:5000, NeuroMab K28/43), gephyrin (1:1000, BD Transduction Labs 610585), β-tubulinIII (1:30,000, Sigma T2200), Cox1 (1:1000, Thermo Scientific PA5-26688), Tecpr1 (1:2000, Cell Signaling D6C10), Atg5–12 (1:1000, Cell Signaling D1G9), and Atg7 (1:2500, R&D Systems MAB6608). Band densitometry was quantified using ImageJ software on unaltered images, and normalized to total protein loaded using ponceau stain, unless otherwise noted. All samples were run at least twice to confirm that the assay was consistent and that the observed effect was replicable; each data point represents the average of two independent blot results for one animal.

To assess the levels of prefibrillar and fibrillar oligomers, we used the conformation specific antibodies A11 (Invitrogen AHB0052) and OC (Millipore AB2286), respectively [30]. Levels of oligomers were normalized to total Aβ using the 4G8 antibody (Biolegend 800701). We homogenized cortex tissue in PBS + 1× Halt protease inhibitor (Thermo Fisher) at 4.5 months of age, when AP mice have visible plaque, but cTAP mice do not. Homogenates were centrifuged at 100,000×*g* to isolate soluble oligomers [30], and supernatant was spotted onto membranes for standard dot blotting procedures.

Immunohistochemistry and immunofluorescence

After fixation, brain hemispheres were transferred to fresh PBS for 24 h, 2×. Hemispheres were embedded in paraffin, sectioned in 10-μm serial sections, then de-paraffinized and rehydrated. Antigen retrieval was performed in 10 mM sodium citrate by boiling for 5 min, and then, endogenous peroxidases were inactivated with 0.3% sodium hydroxide for 30 min, either after antigen retrieval or after application of the primary antibody. Slides were blocked in 5% or 1.5% normal goat serum with 0.1% triton x-100, or using the mouse on mouse staining kit (Vector Labs BMK-2202). Primary antibodies used were: 4G8 (1:1000, BioLegend 800702), TDP-43 N-terminal (1:500, Proteintech 10782-2-AP), TDP-43 C-

terminal (1:150, Proteintech 12892-1-AP), SMI-31 (1:2000 IHC/1:1200 IF, Biolegend smi-31r), and cleaved caspase-3 (Cell Signaling Technology D3E9). Secondary antibodies were either biotinylated for subsequent avidin binding and diaminobenzidine (DAB) reaction, or were conjugated to fluorescent epitopes (Alexa Fluor 488, 555, or 564, 1:200). DNA fragmentation was detected using an in situ TUNEL assay (Trevigen). Hematoxylin, cresyl violet, or DAPI were used as nuclear counterstains. Brightfield images were taken on an Olympus brightfield microscope with a ProgRes C14 Plus digital camera and Progres CapturePro imaging software. Immunofluorescent images were taken on a Zeiss LSM 510 confocal microscope using a 63× oil objective in the Multiphoton Imaging Core of the Johns Hopkins School of Medicine, Department of Neuroscience. An Argon/2 laser was used for 488-nm detection (transmission 24.8%, gain 541, amplifier offset −0.017), and a DPSS laser was used for 561-nm detection (transmission 37.8%, gain 621, amplifier offset −0.062).

Stereology

Brain volume, plaque burden, and neuron counts were assessed using unbiased stereological methods with Stereo Investigator software. Brain region volumes were estimated using the Cavalieri probe (counting frame 150 × 150 μm, grid spacing 200 μm) in three sections/animal spaced 360 μm apart. Plaque burden was estimated using the Area Fraction Fractionator probe (counting frame: cortex 300 × 350 μm, cerebellum and hippocampus 200 × 250 μm, grid spacing 15 μm) in three sections/animal spaced 360 μm apart. Neuron counts of hippocampal areas CA3/2, CA1 and DG were estimated by counting the number of neuron nuclei per region in ten sections/animal spaced 150 μm apart. As all tissue was cut in 10-μm-thin sections, an optical disector method was not used; however, these hippocampal layers and neuronal nuclei sizes are highly uniform, which minimizes the caveats of using profile counting.

RNA sequencing functional analysis

RNA sequencing data from the forebrains of 3-month *CaMKIIα-Cre*^{ER};*Tdp-43*$^{F/F}$ mice was obtained from Jeong et al. (in review). To generate a list of the cryptic exon-associated genes most likely to exert a functional effect in neurons after depletion of TDP-43, those with an absolute RNA fold change greater than 1.5 were included. Fold changes of lesser magnitude are unlikely to exert a functional outcome on the cell and were not included. This selection criterion reduced the list from >100 transcripts to 11 (Table 1). The functional pathways of the corresponding genes in neurons were determined using GeneCards and verified by a manual literature search.

Elevated plus maze

The elevated plus maze (San Diego Instruments) test was performed to evaluate levels of anxiety-like behavior. This maze was made of stainless steel and consisted of two closed arms measuring 19.5 inches in length × 4 inches in width × 15.5 inches in height and two open arms measuring 19.5 inches in length × 4 inches in width. These arms were connected by a 4 × 4-inch platform. Each mouse was placed on the center platform and remained in the maze for 5 min. Number of visits and time spent in the closed arms and open arms was measured.

Y-maze task

The Y-maze has three arms (18.5 inches in length × 2.5 inches in width × 1 inch in height) radiating at equal angles from a central platform. Mice were place into the end of one arm and allowed to explore freely for 5 min. The sequence of arm entries was recorded. The spontaneous alternation behavior was calculated as the number of triads containing entries into all three arms divided by the maximum possible alternations.

Randomization and blinding

All animals received tamoxifen treatment. No randomization was used to assign animals to groups for data collection and processing. Rather, animals of each genotype were collected at the appropriate age in batches containing approximately equal representation of each genotype. Tissue from each age group was processed in a single batch when possible, or in multiple batches containing equal numbers of animals from each genotype. During data collection and analysis, the investigator was blinded to genotype by assigning an unrelated individual number to each animal at weaning.

Statistical analysis

Sample power calculations were performed using SPSS Sample Power 3.0. To measure mean differences of at least 25% with an estimated standard deviation of 15%, a per group sample size of 8 animals has an estimated 87% power. For larger mean differences of at least 40%, a per group sample size of 5 animals has an estimated 96% power. Therefore, for most statistical analyses, the final sample sizes are $n > 8$, and all are $n \geq 5$ mice/group.

Data were collected in Excel (Microsoft) and organized and analyzed with SPSS Statistics 23.0 (IBM) using univariate ANOVA by genotype within each age group. Boxplots show the median, interquartile range (box) 1.5 interquartile range (whiskers), outliers (○), and extreme cases (◇) of individual variables for each genotype. Normality was validated by ensuring that the |skew/standard error skew| <2 for each group, and Welch's test was used if normality was violated in one or more groups. When dependent variables were found significant across genotypes, we used Gabriel post hoc test (robust to slightly unequal sample sizes), or Games-Howell (robust to violations of homogeneity of variances). Post hoc comparisons are paired with “wt”, unless otherwise specified. Unpaired *t* tests (two-tailed) are reported when only two groups are compared. For linear regression analysis, R^2 values and ANOVA significance values are reported. For correlation analysis, Spearman's rho values for correlation strength and two-tailed significance values are reported. For all studies, no data points were removed from analysis.

Figure generation

Figures were generated using SPSS Statistics 23.0 (IBM), Adobe Illustrator, and CoreIDraw.

Results

Certain pyramidal neurons are selectively vulnerable to depletion of TDP-43 in the forebrain

It has long been recognized that certain large pyramidal neurons of the hippocampus and frontal cortex are selectively vulnerable to neurodegeneration in AD [43, 53]. To determine whether these neuronal populations are also more sensitive to depletion of TDP-43, we depleted TDP-43 in the forebrain (Fig. 1a) and examined the hippocampus and cortical layers. Administration of tamoxifen in adult cT mice led to depletion of TDP-43 in 80% of pyramidal neurons in the hippocampus and cortical layers II/III and IV, and in 40% of neurons in cortical layers V and VI (Fig. 1b–d). The difference in TDP-43 depletion between upper and lower cortical layers is consistent with previous work showing that the promoter used in this study, *CaMKIIα*, is expressed most strongly in the hippocampus and cortical layers II/III and IV, with relatively weak expression in layers V and VI (Allen Brain Atlas experiment 79360274, NCBI accession # NM_009792.1; mouse.brain-map.org).

Depletion of TDP-43 led to progressive age-dependent forebrain atrophy in the hippocampus, cortex, and corpus callosum (Fig. 2a, b). As expected, the volume of the cerebellum remained normal (Fig. 2b), since TDP-43 is not depleted in this region. While TDP-43 has been identified as an essential gene in mammals [9, 56], we found that not all neurons in the mature mouse forebrain are equally vulnerable to depletion of TDP-43. Rather, we observed early selective vulnerability in hippocampal CA3/2 (Fig. 2c, d) and cortical layers III and V neurons (Fig. 2e, f) at 3 months of age judged by visual inspection of degenerative morphology and counting of healthy neurons on CV stained slides. Notably, cortical layers III and V are also selectively vulnerable in AD and their degeneration correlates with cognitive decline early in the disease [43, 52]. In addition, pathological accumulation of phosphorylated neurofilament [39] was evident only in layer V neurons lacking TDP-43 as early as 3 months (Fig. 2g, h) and >50% of layer V neurons degenerated by 4 months of age [$t(10) = 7.029$, $p < 0.001$, wt ($M = 868$, SD = 78), cT ($M = 385$, SD = 137), n: wt = 5, ct = 7]. Despite these changes in neurofilament, we found no evidence that tau phosphorylation or aggregation was affected in cT mice up to 9 months of age, either by immunostaining or immunoblot with the tau phospo-202/205 antibody AT8 (ThermoFisher) (not shown).

Depletion of TDP-43 leads to cognitive and behavioral abnormalities in cT mice

The cognitive profile for ALS-FTD includes disinhibition [50] and deficits in hippocampal dependent memory that have been traditionally considered characteristic of Alzheimer's disease [13, 19, 47]. Therefore, we tested male and female cT and wt mice using the elevated plus maze and spontaneous alternation in the Y-maze, which assess these parameters of cognitive function, respectively. We find that cT mice exhibit poor performance in the spontaneous alternation task in the Y-maze by 6 months of age (Fig. 2i, middle), indicative of hippocampal dependent memory deficits. Later, by 14 months of age, cT mice also spend significantly more time in the open arm of the elevated plus maze, indicating disinhibition or reduced anxiety (Fig. 2i, left). We found no differences between male and female mice in either task (data not shown). In addition, these differences are not

associated with any mobility impairment, as the total number of arm entries did not differ between cT and wt mice even at 14 months of age (Fig. 2i, right). Together, these data suggest that TDP-43 depletion in the mouse forebrain leads to cognitive deficits analogous to those seen in ALS-FTD, and to some extent in AD.

Depletion of TDP-43 exacerbates neurodegeneration in the hippocampus of *APP$_{swe}$/PS1ΔE9* mice

Previous work has shown that TDP-43 proteinopathy in AD cases correlates strongly with worsened neurodegeneration and cognition [27]. However, it remains unclear whether nuclear depletion of TDP-43 exacerbates neurodegeneration in this case, or whether it merely occurs alongside these deficits. To assess whether nuclear depletion of TDP-43 might exacerbate neurodegeneration in AD, we crossed *CaMKIIα-Cre^{ER};Tdp-43$^{F/F}$* (cT) mice with AD-linked *APP$_{swe}$/PS1ΔE9* (AP) mice to generate *APP$_{swe}$/PS1ΔE9* mice lacking *Tdp-43* in forebrain neurons (cTAP) (Fig. 3a). As noted above, though *APP$_{swe}$/PS1ΔE9* mice lack frank neuron loss, they exhibit significant synaptic and mitochondrial degeneration [12, 68], pathological features that are well suited to assess exacerbated neurodegeneration in an AD-related context. As expected, the expression of *APP$_{swe}$/PS1ΔE9* had no additional effect on the rate of *Tdp-43* excision [Ctx L5 $F(1,9) = 1.872$, $p = 0.204$].

We performed TUNEL staining to label DNA breaks indicative of neurons that have initiated processes of cell death. Consistent with the pattern of degeneration identified by CV stain (Fig. 2c–f), TUNEL staining was found in hippocampal CA3 pyramidal neurons and cerebral cortex layers III and VI in cT and cTAP mice at 3 months of age (Fig. 3b, left). Quantification of TUNEL staining in the CA3 of 8-month mice shows significantly more TUNEL positive neurons in cT and cTAP mice compared to AP littermates (Fig. 3c). Though there is a trend of increased TUNEL staining in cTAP mice compared to cT littermates at this age, it did not reach significance. Notably, the selective degeneration observed in cT and cTAP mice does not appear to involve caspase-3 as a cell death executioner [14], as cleaved caspase-3 was not detected in the cell bodies of hippocampal (Fig. 3b, right) or cortical pyramidal neurons (data not shown) at 3 or 8 months of age. However, we found numerous cleaved caspase-3 positive punctae in the CA1 stratum radiatum of 8-month-old cTAP mice, while only occasional punctae appear in this region in cT mice and no staining is evident in AP mice (Fig. 3d). Notably, a large body of evidence demonstrates that caspase-3 also has roles in synaptic plasticity, learning, and memory when activated locally at synapses (reviewed in [10, 59]). This body of work suggests that the caspase-3 staining we observe in the CA1 stratum radiatum may represent an attempted adaptive response by CA1 neurons, or could be a result of a prolonged degenerative process of the CA3 Schaffer collateral axon terminals that project to this area.

Further histological and electron microscopic analysis of the CA1 revealed numerous pyramidal neurons with markedly swollen, empty cytoplasm in cTAP mice compared to control littermates, suggesting degenerating neurons (Fig. 3c). In addition, some cTAP animals also showed occasional darkly stained pyknotic cells within the CA1 layer (Fig. 3c, left, arrow) and severe vacuolation of the stratum radiatum (not shown), while these

abnormalities were absent from cT and AP mice. Exacerbated neurodegeneration in cTAP mice was further confirmed by morphological analysis, judged by severe swelling and dystrophy in mitochondria and Golgi/ER, and cytoplasmic discontinuity with loss of ribosomes (Fig. 3c, middle, right).

We showed previously that depletion of TDP-43 leads to the incorporation of aberrant cryptic exons, and usually to subsequent degradation of the associated mRNAs [36]. In addition, we previously analyzed the effects of cryptic exon incorporation on the transcriptome in 3-month-old *CaMKIIα-Cre*^{ER};*Tdp-43*$^{F/F}$ mice compared to controls (Jeong et al., in review). Here, we harness this resource to investigate the functional pathways of cryptic exon-associated RNAs most likely to exert a meaningful effect on mature neurons. We selected cryptic exon-associated RNAs with absolute fold change >1.5, corresponding to the ~10% most strongly affected in the dataset. We then identified the functional pathways of these RNAs using the GeneCards database followed by verification with manual literature searches. Importantly, we identified three pathways strongly implicated in the pathogenesis of AD that are also affected by cryptic exon incorporation in cT mice: synaptic signaling [18, 58], mitochondrial function [68, 70], and autophagy [45] (Table 1). Therefore, we examined the following key components of these three essential pathways to confirm exacerbated neurodegeneration at the molecular level in the hippocampus of cTAP mice.

Importantly, in mitochondrial function, autophagy, and synaptic signaling, we find evidence of exacerbated neurodegeneration in the hippocampus of cTAP mice compared to AP and cT littermates. In mitochondria, we observed a significant loss of Cox1, an essential component of the electron transport chain, in cTAP mice compared to littermate controls (Fig. 4a, b). This is consistent with previous findings that TDP-43 regulates mitochondrial dynamics and that its loss reduces mitochondrial fission [66], as blocking fission experimentally has been shown to reduce mitochondrial respiration and ATP production [46]. In the autophagy pathway, we previously reported that *Tecpr1*, which encodes a protein critical for the fusion of autophagosomes to lysosomes [8], is a major target of TDP-43 in the brain [Jeong et al. in review]. As expected, protein levels of Tecpr1 were reduced in cT and cTAP mice lacking TDP-43 [3 months: $F(3,10) = 13.450$, ***$p = 0.001$, Gabriel wt vs. cT *$p = 0.011$, wt vs. cTAP *$p = 0.016$; 8 months: $F(3,19) = 6.149$, ***$p = 0.004$, Gabriel wt vs. cT **$p = 0.007$, wt vs. cTAP *$p = 0.020$, blot shown Fig. 4d]. Tecpr1 binds the Atg5–12 complex [8, 24], and depletion of Atg5 has been shown to cause neurodegeneration in vivo [16]. Notably, Atg5–12 was also reduced in cTAP mice compared to littermate controls by 8 months (Fig. 4c, d), while another essential autophagosome formation factor that is not a Tecpr1 binding partner (Atg7) remained unchanged (Fig. 4d, [Welch(3,9.619) = 1.680, $p = 0.236$]). The apparent specificity of the Atg5–12 down-regulation suggests that some TDP-43-associated cryptic exons may impair neuronal function directly. Finally, the pre-synaptic vesicle protein synaptophysin and the neuron cell body and axonal cytoskeletal marker β-tubulin-III were reduced in cTAP mice by 8 months compared to littermate controls (Fig. 4e, f). Interestingly, cTAP mice did not exhibit significant differences in post-synaptic excitatory (PSD-95) or inhibitory receptor scaffolds (gephyrin [$F(3,20) = 0.458$, $p = 0.715$]) by 8 months, though PSD95 was significantly increased in all transgenic genotypes [Welch(3,9.648) = 40.973, $p < 0.001$; Games-Howell AP ***$p < 0.001$, cT **$p = 0.002$, and cTAP **$p = 0.007$] (Fig. 4f). These findings are consistent with observations that presynaptic terminals are initially

affected in the cases of AD and that this loss correlates with cognitive decline [55, 61]. Together, the significant loss of key markers of the essential neuronal pathways investigated contribute further evidence of exacerbated neurodegeneration in the hippocampus of double transgenic AD-linked mutant mice lacking TDP-43 in their forebrain neurons compared to single transgenic littermate controls. These findings suggest that depletion of TDP-43 does contribute to neurodegeneration in cases of AD with TDP-43 proteinopathy, and is not merely a bystander of the degenerative process.

Exacerbated neurodegeneration in *APP_{swe}/PS1ΔE9* mice lacking TDP-43 in the forebrain correlates with increased pre-fibril, but not fibril or plaque Aβ

Unexpectedly, while depletion of TDP-43 in *APP_{swe}/PS1ΔE9* mice exacerbated neurodegeneration, it also significantly reduced Aβ plaque burden (Fig. 5a, b). In contrast, the relative level of pre-fibril oligomers was significantly increased compared to fibril oligomers in forebrain homogenates of cTAP compared to AP mice by 4 months (Fig. 5c, d). These data indicate that the exacerbated neurodegeneration occurring in cTAP mice is independent of Aβ plaque burden or their fibril oligomer precursors, but is instead associated with more soluble pre-fibril oligomers. Indeed, we found that the levels of pre-fibril [Spearman's rho $\rho = -0.697$, $p = 0.025$, $n = 10$, power = 77%], but not fibril [Spearman's rho $\rho = -0.406$, $p = 0.244$, $n = 10$] oligomers correlated significantly with lower synaptophysin levels at 8 months (Fig. 5e, f). Importantly, the total levels of Aβ42 were unchanged (Fig. 5g), as well as levels of the Aβ precursor protein (APP) [$F(1,11) = 0.164$, $p = 0.694$] and its proteolytic enzymes PS1 [$F(1,6) = 1.540$, $p = 0.261$] and BACE1 [$F(1,6) = 0.004$, $p = 0.950$] in cTAP mice compared to AP littermates. Finally, simple linear regression for dependence modeling demonstrated that the reduced plaque density was not significantly explained by the volume loss observed in cTAP mice (Fig. 5h). Together, these findings indicate that the reduced burden of fibrillar and plaque Aβ is not due to changes in Aβ production, and may instead reflect an important mechanistic effect of TDP-43 depletion on Aβ oligomerization dynamics.

Discussion

Previous work established an essential role for TDP-43 in mammalian embryogenesis [34, 56] and vertebrate development [54], as well as diverse roles during adulthood [9] including neuron survival in the spinal cord [23, 67, 69]. We now show that in adult mammals depletion of TDP-43 is not equally toxic to all populations of forebrain neurons, and frontal cortex layers III and V and hippocampal CA3/2 pyramidal neurons are selectively vulnerable. This suggests that the mechanisms underlying neuronal death during development and adulthood are likely to be highly dissimilar, and indicate caution when applying evidence from constitutive or developmentally based models of TDP-43 dysfunction to the neurodegenerative disease state. Our findings are consistent with studies in mice expressing human TDP-43 with a mutated nuclear localization sequence in the forebrain, which showed similar selective vulnerability [22] as well as cognitive and behavioral deficits [1]. The vulnerability of cortical layer V neurons is particularly striking given that a lower percentage of these neurons lose TDP-43 after tamoxifen treatment compared to the upper layers. Therefore, determining whether depletion of TDP-43 is

associated with similar selective vulnerability patterns in humans may have therapeutic relevance, and would provide important information about the translational potential and limitations of various mouse models. However, the design and interpretation of selective vulnerability studies in human disease may be complicated by the fact that TDP-43 proteinopathy occurs only in a small subset of neurons that appear unequally distributed throughout hippocampal sub-regions [29, 64]. Therefore, experiments will need to be carefully devised to asses this question.

Interestingly, the stratum radiatum of the CA1, containing densely packed dendrites of the pyramidal neurons of this layer, showed strong staining of activated caspase-3 in cTAP mice at 8 months. The precise subcellular localization of this staining is not identified here. As CA1 neurons are uniquely spared within the hippocampus up to at least 14 months of age, the staining of caspase-3 in the stratum radiatum containing the dendrites from these neurons may be indicative of an attempted protective or adaptive response allowing their prolonged survival compared to other hippocampal pyramidal neurons. This view is consistent with a large body of evidence that activated caspase-3 has roles in synaptic plasticity and memory when activated locally at synapses (reviewed in [10, 59]), and that this local activation leads to adaptive glutamate receptor cleavage under excitotoxic conditions [38]. Alternatively, the caspase-3 staining could be contained in the synaptic terminals of Schaffer collateral axons emanating from the degenerated CA3 region [7, 42]. These terminals could be derived from the residual CA3 pyramidal neurons, since generally about 50% are lost. Interestingly, our finding that caspase-3 staining was much more pronounced in cTAP than cT mice suggests that Aβ and loss of TDP-43 may provoke a common caspase-mediated pathway in the CA1. Our findings that presynaptic synaptophysin is reduced, while postsynaptic scaffolds PSD-95 and gephyrin are increased further suggest that an adaptive or reactive mechanism may indeed be at work. Further study may reveal an adaptive mechanism employed by CA1 neurons which could be exploited to protect other neurons under conditions of abnormal Aβ and loss of nuclear TDP-43.

Together, our findings support a model whereby nuclear depletion of TDP-43 contributes to the pathogenesis of AD in cases with TDP-43 proteinopathy. We show evidence that key components of multiple essential neuronal pathways are significantly reduced at the protein level in the hippocampi of AD-linked mutant mice lacking TDP-43 compared to either AD mutants or TDP-43 depleted mice alone. In addition, while neurons of the hippocampal CA1 region are spared in TDP-43 depleted or AD-linked mutant mice alone, they show multiple morphological features of degeneration in mice with both genetic alterations. These findings strongly support the hypothesis that nuclear depletion of TDP-43 contributes to the pathogenesis of disease in patients with TDP-43 proteinopathy, rather than being a bystander in the degenerative process. Importantly, we also find that the number of TUNEL positive neurons is not significantly different between cT and cTAP mice at 8 months of age, and that the nuclei of these neurons are not positive for activated caspase-3. This suggests that although the neurodegenerative process is accelerated and worsened by the presence of mutant APP, it does not terminate quickly in neuron death. This interpretation is consistent with the long course of disease in Alzheimer's patients with TDP-43 proteinopathy. Interestingly, our findings in the autophagy pathway also support the hypothesis that TDP-43-associated cryptic exons may affect some neuronal functions directly, as

autophagosome proteins that interact with the cryptic exon-associated Tecpr1 were reduced, while those that do not remained unchanged. This suggests that continued studies on the functional effects of cryptic exons in mature neurons may be of therapeutic relevance. In addition, our findings provide strong rationale to develop novel therapeutics to alleviate the depletion of nuclear TDP-43 and to create functional antemortem biomarkers to detect loss of TDP-43 function.

Our studies also revealed an unexpected interaction between depletion of TDP-43 and Aβ aggregation. Specifically, depletion of TDP-43 increased soluble prefibril Aβ oligomers while reducing plaques and fibril oligomers. As neurodegeneration was also worsened in these mice, our data are consistent with the view that non-fibrillar soluble forms of Aβ, rather than fibrils and plaques, facilitate neurodegeneration in AD [32, 41]. Indeed, we found a significant inverse correlation between prefibril Aβ oligomers and the presynaptic marker synaptophysin, while fibril Aβ was uncorrelated. Because the antibodies used to measure pre-fibril and fibril oligomers in this study have been shown to bind to amyloid oligomers composed of various proteins including α-synuclein [30], examining whether these other proteins are similarly affected by the loss of TDP-43 may be of interest. However, in this study, the overexpression of mutant APP in our mouse model makes it very likely that the large majority of the signal is due to Aβ. Given the apparent importance of the conformational state of Aβ to its neurodegenerative toxicity, the equilibrium relationship between different conformational states underscores a great challenge of designing effective Aβ-directed therapeutics [51]. However, interim clinical trial data from the “second generation” Aβ-directed antibodies derived from aged cognitively normal humans, such as Aducanumab (BIIB037), appear promising [57]. Clinico-pathologic studies of aging suggest that TDP-43 and Aβ pathology formation are independent events [33] and that nuclear depletion of TDP-43 may occur in a majority of AD cases [27]. Therefore, our findings suggest that stratifying AD subjects by the presence of TDP-43 pathology and associated cryptic exons may empower clinical trials of Aβ-directed (and possibly also tau-directed) therapeutics.

Finally, our findings indicate that depletion of TDP-43 and pre-fibril Aβ interact to exacerbate neurodegenerative processes, and suggest that further studies investigating the underlying mechanisms would be worthwhile. In addition, TDP-43 proteinopathy encompasses both its depletion from the nucleus and its long-term localization to the cytoplasm in potentially toxic aggregates. Here, we have modeled only the facet of nuclear depletion to allow isolated investigation of its effects without the potentially confounding influence of cytoplasmic aggregates. However, future work in models that also recapitulate aspects of cytoplasmic aggregation may provide additional important insights into the disease state, such as potential aggregative “cross–seeding” interactions between TDP-43 and Aβ [15].

Acknowledgements

This work was supported in part by the Johns Hopkins University School of Medicine Neuropathology Frederick J. Pelda Alzheimer's Research Fund, the Robert Packard Center for ALS Research, the Amyotrophic Lateral Sclerosis Association, National Institute of Health grants R01-NS095969 and R01-NS079348, and the Johns Hopkins

Alzheimer's Disease Research Center (P50AG05146). The authors wish to thank Venette Nehus and Barbara Smith for technical assistance.

References

1. Alfieri JA, Pino NS, Igaz LM. reversible behavioral phenotypes in a conditional mouse model of TDP-43 proteinopathies. J Neurosci. 2014; 34:15244–15259. doi:10.1523/JNEUROSCI.1918-14.2014. [PubMed: 25392493]
2. Alzheimer's Association. 2016 Alzheimer's disease facts and figures. Alzheimer's & Dementia. 2016; 12(4):459–509.
3. Amador-Ortiz C, Lin W-L, Ahmed Z, Personett D, Davies P, Duara R, Graff-Radford NR, Hutton ML, Dickson DW. TDP-43 immunoreactivity in hippocampal sclerosis and Alzheimer's disease. Ann Neurol. 2007; 61:435–445. doi:10.1002/ana.21154. [PubMed: 17469117]
4. Andrade-Moraes CH, Oliveira-Pinto AV, Castro-Fonseca E, da Silva CG, Guimarães DM, Szczupak D, Parente-Bruno DR, Carvalho LRB, Polichiso L, Gomes BV, Oliveira LM, Rodriguez RD, Leite REP, Ferretti-Rebustini REL, Jacob-Filho W, Pasqualucci CA, Grinberg LT, Lent R. Cell number changes in Alzheimer's disease relate to dementia, not to plaques and tangles. Brain. 2013; 136:3738–3752. doi:10.1093/brain/awt273. [PubMed: 24136825]
5. Beach TG, Monsell SE, Phillips LE, Kukull W. Accuracy of the clinical diagnosis of Alzheimer disease at National Institute on Aging Alzheimer Disease Centers, 2005–2010. J Neuropathol Exp Neurol. 2012; 71:266–273. doi:10.1097/NEN.0b013e31824b211b. [PubMed: 22437338]
6. Burgess BL, McIsaac SA, Naus KE, Chan JY, Tansley GHK, Yang J, Miao F, Ross CJD, van Eck M, Hayden MR, van Nostrand W, St George-Hyslop P, Westaway D, Wellington CL. Elevated plasma triglyceride levels precede amyloid deposition in Alzheimer's disease mouse models with abundant A beta in plasma. Neurobiol Dis. 2006; 24:114–127. doi:10.1016/j.nbd.2006.06.007. [PubMed: 16899370]
7. Calhoun ME, Jucker M, Martin LJ, Thinakaran G, Price DL, Mouton PR. Comparative evaluation of synaptophysin-based methods for quantification of synapses. J Neurocytol. 1996; 25:821–828. doi:10.1007/BF02284844. [PubMed: 9023727]
8. Chen D, Fan W, Lu Y, Ding X, Chen S, Zhong Q. A Mammalian autophagosome maturation mechanism mediated by TECPR1 and the Atg12-Atg5 conjugate. Mol Cell. 2012; 45:629–641. doi:10.1016/j.molcel.2011.12.036. [PubMed: 22342342]
9. Chiang P-M, Ling J, Jeong YH, Price DL, Aja SM, Wong PC. Deletion of TDP-43 down-regulates Tbc1d1, a gene linked to obesity, and alters body fat metabolism. Proc Natl Acad Sci. 2010; 107:16320–16324. doi:10.1073/pnas.1002176107. [PubMed: 20660762]
10. D'Amelio M, Cavallucci V, Cecconi F. Neuronal caspase-3 signaling: not only cell death. Cell Death Differ. 2010; 17:1104–1114. doi:10.1038/cdd.2009.180. [PubMed: 19960023]
11. Davis D, Schmitt F, Wekstein D, Markesbery W. Alzheimer neuropathologic alterations in aged cognitively normal subjects. J Neuropathol Exp Neurol. 1999; 58:376–388. [PubMed: 10218633]
12. Fernandez-Martos CM, King AE, Atkinson RAK, Woodhouse A, Vickers JC. Neurofilament light gene deletion exacerbates amyloid, dystrophic neurite and synaptic pathology in the APP/PS1 transgenic model of Alzheimer's disease. Neurobiol Aging. 2015; 36:2757–2767. doi:10.1016/j.neurobiolaging.2015.07.003. [PubMed: 26344875]
13. Frisch S, Dukart J, Vogt B, Horstmann A, Becker G, Villringer A, Barthel H, Sabri O, Müller K, Schroeter ML. Dissociating memory networks in early Alzheimer's disease and frontotemporal lobar degeneration—a combined study of hypometabolism and atrophy. PLoS One. 2013 doi:10.1371/journal.pone.0055251.
14. Galluzzi L, Bravo-San Pedro JM, Vitale I, Aaronson SA, Abrams JM, Adam D, Alnemri ES, Altucci L, Andrews D, Annicchiarico-Petruzzelli M, Baehrecke EH, Bazan NG, Bertrand MJ, Bianchi K, Blagosklonny MV, Blomgren K, Borner C, Bredesen DE, Brenner C, Campanella M, Candi E, Cecconi F, Chan FK, Chandel NS, Cheng EH, Chipuk JE, Cidlowski JA, Ciechanover A, Dawson TM, Dawson VL, De Laurenzi V, De Maria R, Debatin K-M, Di Daniele N, Dixit VM, Dynlacht BD, El-Deiry WS, Fimia GM, Flavell RA, Fulda S, Garrido C, Gougeon M-L, Green DR, Gronemeyer H, Hajnoczky G, Hardwick JM, Hengartner MO, Ichijo H, Joseph B, Jost PJ, Kaufmann T, Kepp O, Klionsky DJ, Knight RA, Kumar S, Lemasters JJ, Levine B, Linkermann A,

Lipton SA, Lockshin RA, López-Otín C, Lugli E, Madeo F, Malorni W, Marine J-C, Martin SJ, Martinou J-C, Medema JP, Meier P, Melino S, Mizushima N, Moll U, Muñoz-Pinedo C, Nuñez G, Oberst A, Panaretakis T, Penninger JM, Peter ME, Piacentini M, Pinton P, Prehn JH, Puthalakath H, Rabinovich GA, Ravichandran KS, Rizzuto R, Rodrigues CM, Rubinsztein DC, Rudel T, Shi Y, Simon H-U, Stockwell BR, Szabadkai G, Tait SW, Tang HL, Tavernarakis N, Tsujimoto Y, Vanden Berghe T, Vandenabeele P, Villunger A, Wagner EF, Walczak H, White E, Wood WG, Yuan J, Zakeri Z, Zhivotovsky B, Melino G, Kroemer G. Essential versus accessory aspects of cell death: recommendations of the NCCD 2015. Cell Death Differ. 2014 doi:10.1038/cdd.2014.137.

15. Guerrero-Muñoz MJ, Castillo-Carranza DL, Krishnamurthy S, Paulucci-Holthauzen AA, Sengupta U, Lasagna-Reeves CA, Ahmad Y, Jackson GR, Kayed R. Amyloid-β oligomers as a template for secondary amyloidosis in Alzheimer's disease. Neurobiol Dis. 2014; 71:14–23. doi:10.1016/j.nbd.2014.08.008. [PubMed: 25134727]
16. Hara T, Nakamura K, Matsui M, Yamamoto A, Nakahara Y, Suzuki-Migishima R, Yokoyama M, Mishima K, Saito I, Okano H, Mizushima N. Suppression of basal autophagy in neural cells causes neurodegenerative disease in mice. Nature. 2006; 441:885–889. doi:10.1038/nature04724. [PubMed: 16625204]
17. Herrup K. The case for rejecting the amyloid cascade hypothesis. Nat Neurosci. 2015; 18:794–799. doi:10.1038/nn.4017. [PubMed: 26007212]
18. Holtzman DM, Morris JC, Goate AM. Alzheimer's disease: the challenge of the second century. Sci Transl Med. 2011; 3:77sr1. [PubMed: 21471435]
19. Hornberger M, Piguet O, Graham AJ, Nestor PJ, Hodges JR. How preserved is episodic memory in behavioural variant frontotemporal dementia. Neurology. 2010; 74:473–479.
20. Hu F, Padukkavidana T, Vægter CB, Brady OA, Zheng Y, Mackenzie IR, Feldman HH, Nykjaer A, Strittmatter SM. Sortilin-mediated endocytosis determines levels of the fronto-temporal dementia protein, progranulin. Neuron. 2010; 68:654–667. doi:10.1016/j.jsbmb.2011.07.002.Identification. [PubMed: 21092856]
21. Hyman BT, Gomez-Isla T. Alzheimer's disease is a laminar, regional, and neural system specific disease, not a global brain disease. Neurobiol Aging. 1994; 15:353–354. [PubMed: 7936060]
22. Igaz LM, Kwong LK, Lee EB, Chen-Plotkin A, Swanson E, Unger T, Malunda J, Xu Y, Winton MJ, Trojanowski JQ, Lee VMY. Dysregulation of the ALS-associated gene TDP-43 leads to neuronal death and degeneration in mice. J Clin Invest. 2011; 121:726–738. doi:10.1172/JCI44867. [PubMed: 21206091]
23. Iguchi Y, Katsuno M, Niwa J, Takagi S, Ishigaki S, Ikenaka K, Kawai K, Watanabe H, Yamanaka K, Takahashi R, Misawa H, Sasaki S, Tanaka F, Sobue G. Loss of TDP-43 causes age-dependent progressive motor neuron degeneration. Brain. 2013; 136:1371–1382. doi:10.1093/brain/awt029. [PubMed: 23449777]
24. Inoue K, Rispoli J, Kaphzan H, Klann E, Chen EI, Kim J, Komatsu M, Abeliovich A. Macroautophagy deficiency mediates age-dependent neurodegeneration through a phospho-tau pathway. Mol Neurodegener. 2012; 7:48. doi:10.1186/1750-1326-7-48. [PubMed: 22998728]
25. International Parkinson Disease Genomics Consortium. Imputation of sequence variants for identification of genetic risks for Parkinson's disease: a meta-analysis of genome-wide association studies. Lancet. 2011; 377:641–649. PubMed—NCBI. [PubMed: 21292315]
26. Jeong Y-H, Ling JP, Lin S, Donde A, Braunstein K, Majounie E, Traynor BJ, LaClair KD, Lloyd TE, Wong PC. Tdp-43 cryptic exons are highly variable between cell types. Proc Natl Acad Sci. 2016 in review.
27. Josephs KA, Whitwell JL, Weigand SD, Murray ME, Tosakul-wong N, Liesinger AM, Petrucelli L, Senjem ML, Knopman DS, Boeve BF, Ivnik RJ, Smith GE, Jack CR, Parisi JE, Petersen RC, Dickson DW. TDP-43 is a key player in the clinical features associated with Alzheimer's disease. Acta Neuropathol. 2014; 127:811–824. doi:10.1007/s00401-014-1269-z. [PubMed: 24659241]
28. Josephs KA, Murray ME, Whitwell JL, Parisi JE, Petrucelli L, Jack CR, Petersen RC, Dickson DW. Staging TDP-43 pathology in Alzheimer's disease. Acta Neuropathol. 2014; 127:441–450. doi:10.1007/s00401-013-1211-9. [PubMed: 24240737]
29. Kadokura A, Yamazaki T, Lemere CA, Takatama M, Okamoto K. Regional distribution of TDP-43 inclusions in Alzheimer disease (AD) brains: their relation to AD common pathology. Neuropathology. 2009; 29:566–573. doi:10.1111/j.1440-1789.2009.01017.x. [PubMed: 19422539]

30. Kayed R, Head E, Sarsoza F, Saing T, Cotman CW, Necula M, Margol L, Wu J, Breydo L, Thompson JL, Rasool S, Gurlo T, Butler P, Glabe CG. Fibril specific, conformation dependent antibodies recognize a generic epitope common to amyloid fibrils and fibrillar oligomers that is absent in prefibrillar oligomers. Mol Neurodegener. 2007; 2:18. doi:10.1186/1750-1326-2-18. [PubMed: 17897471]

31. Kim J, Basak JM, Holtzman DM. The role of apolipoprotein E in Alzheimer's disease. Neuron. 2009; 63:287–303. doi:10.1016/j.neuron.2009.06.026. [PubMed: 19679070]

32. Koffie RM, Meyer-Luehmann M, Hashimoto T, Adams KW, Mielke ML, Garcia-Alloza M, Micheva KD, Smith SJ, Kim ML, Lee VM, Hyman BT, Spires-Jones TL. Oligomeric amyloid beta associates with postsynaptic densities and correlates with excitatory synapse loss near senile plaques. Proc Natl Acad Sci. 2009; 106:4012–4017. doi:10.1073/pnas.0811698106. [PubMed: 19228947]

33. Kovacs GG, Milenkovic I, Wöhrer A, Höftberger R, Gelpi E, Haberler C, Hönigschnabl S, Reiner-Concin A, Heinzl H, Jungwirth S, Krampla W, Fischer P, Budka H. Non-Alzheimer neurodegenerative pathologies and their combinations are more frequent than commonly believed in the elderly brain: a community-based autopsy series. Acta Neuropathol. 2013; 126:365–384. doi:10.1007/s00401-013-1157-y. [PubMed: 23900711]

34. Kraemer BC, Schuck T, Wheeler JM, Robinson LC, Trojanowski JQ, Lee VMY, Schellenberg GD. Loss of murine TDP-43 disrupts motor function and plays an essential role in embryogenesis. Acta Neuropathol. 2010; 119:409–419. doi:10.1007/s00401-010-0659-0. [PubMed: 20198480]

35. LaClair KD, Manaye KF, Lee DL, Allard JS, Savonenko AV, Troncoso JC, Wong PC. Treatment with bexarotene, a compound that increases apolipoprotein-E, provides no cognitive benefit in mutant APP/PS1 mice. Mol Neurodegener. 2013; 8:18. doi:10.1186/1750-1326-8-18. [PubMed: 23764200]

36. Ling JP, Pletnikova O, Troncoso JC, Wong PC. TDP-43 repression of nonconserved cryptic exons is compromised in ALS-FTD. Science (80−). 2015; 349:650–655. doi:10.1126/science.aab0983.

37. Liu R, Yang G, Nonaka T, Arai T, Jia W, Cynader MS. Reducing TDP-43 aggregation does not prevent its cytotoxicity. Acta Neuropathol Commun. 2013 doi:10.1186/2051-5960-1-49.

38. Lu C, Fu W, Salvesen GS, Mattson MP. Direct cleavage of AMPA receptor subunit GluR1 and suppression of AMPA currents by caspase-3: implications for synaptic plasticity and excitotoxic neuronal death. Neuromol Med. 2002; 1:69–79. doi:10.1385/NMM:1:1:69.

39. Martin L, Kaiser A, Price A. Motor neuron degeneration after sciatic nerve avulsion in adult rat evolves with oxidative stress and is apoptosis. J Neurobiol. 1999; 40:185–201. doi:10.1002/(SICI)1097-4695(199908)40:2<185:AID-NEU5>3.0.CO;2-#. [PubMed: 10413449]

40. Morris GP, Clark IA, Vissel B. Inconsistencies and controversies surrounding the amyloid hypothesis of Alzheimer's disease. Acta Neuropathol Commun. 2014; 2:135. doi:10.1186/s40478-014-0135-5. [PubMed: 25231068]

41. Musiek ES, Holtzman DM. Three dimensions of the amyloid hypothesis: time, space and “wingmen”. Nat Neurosci. 2015; 18:800–806. doi:10.1038/nn.4018. [PubMed: 26007213]

42. Nadler JV, Perry BW, Cotman CW. Selective reinnervation of hippocampal area CA1 and the fascia dentata after destruction of CA3-CA4 afferents with kainic acid. Brain Res. 1980; 182:1–9. [PubMed: 7350980]

43. Neary D, Snowden J, Mann D, Bowen D, Sims N, Northen B, Yates P, Davidson A. Alzheimer's disease: a correlative study. J Neurol. 1986; 49:229–237.

44. Neumann M, Sampathu DM, Kwong LK, Truax AC, Micsenyi MC, Chou TT, Bruce J, Schuck T, Grossman M, Clark CM, McCluskey LF, Miller BL, Masliah E, Mackenzie IR, Feldman H, Feiden W, Kretzschmar HA, Trojanowski JQ, Lee VM. Ubiquitinated TDP-43 in frontotemporal lobar degeneration and amyotrophic lateral sclerosis. Science (80−). 2006; 314:130–133. doi:10.1126/science.1134108.

45. Nixon RA. The role of autophagy in neurodegenerative disease. Nat Med. 2013; 19:983–997. doi:10.1038/nm.3232. [PubMed: 23921753]

46. Parone PA, Da Druz S, Tondera D, Mattenberger Y, James DI, Maechler P, Barja F, Martinou JC. Preventing mitochondrial fission impairs mitochondrial function and leads to loss of mitochondrial DNA. PLoS One. 2008; 3:1–9. doi:10.1371/journal. pone.0003257.

47. Pennington C, Hodges JR, Hornberger M. Neural correlates of episodic memory in behavioral variant frontotemporal dementia. J Alzheimers Dis. 2011; 24:261–268. doi:10.3233/JAD-2011-101668. [PubMed: 21239854]
48. Probst A, Tolnay M, Langui D, Goedert M, Spillantini MG. Pick's disease: hyperphosphorylated tau protein segregates to the somatoaxonal compartment. Acta Neuropathol. 1996; 92:588–596. [PubMed: 8960316]
49. Rahimi J, Kovacs GG. Prevalence of mixed pathologies in the aging brain. Alzheimers Res Ther. 2014; 6:1–11. doi:10.1186/s13195-014-0082-1. [PubMed: 24382028]
50. Rascovsky K, Hodges JR, Knopman D, Mendez MF, Kramer JH, Neuhaus J, van Swieten JC, Seelaar H, Dopper EGP, Onyike CU, Hillis AE, Josephs KA, Boeve BF, Kertesz A, Seeley WW, Rankin KP, Johnson JK, Gorno-Tempini M-L, Rosen H, Prioleau-Latham CE, Lee A, Kipps CM, Lillo P, Piguet O, Rohrer JD, Rossor MN, Warren JD, Fox NC, Galasko D, Salmon DP, Black SE, Mesulam M, Weintraub S, Dickerson BC, Diehl-Schmid J, Pasquier F, Deramecourt V, Lebert F, Pijnenburg Y, Chow TW, Manes F, Grafman J, Cappa SF, Freedman M, Grossman M, Miller BL. Sensitivity of revised diagnostic criteria for the behavioural variant of frontotemporal dementia. Brain. 2011; 134:2456–2477. doi:10.1093/brain/awr179. [PubMed: 21810890]
51. Rosenblum WI. Why Alzheimer trials fail: Removing soluble oligomeric beta amyloid is essential, inconsistent, and difficult. Neurobiol Aging. 2014; 35:969–974. doi:10.1016/j.neurobiolaging.2013.10.085. [PubMed: 24210593]
52. Scheff SW, Price DA. Alzheimer's disease-related alterations in synaptic density: neocortex and hippocampus. J Alzheimers Dis. 2006; 9:101–115.
53. Scheff SW, Price DA, Schmitt FA, Mufson EJ. Hippocampal synaptic loss in early Alzheimer's disease and mild cognitive impairment. Neurobiol Aging. 2006; 27:1372–1384. doi:10.1016/j.neurobiolaging.2005.09.012. [PubMed: 16289476]
54. Schmid B, Hruscha A, Hogl S, Banzhaf-strathmann J, Strecker K. Loss of ALS-associated TDP-43 in zebra fish causes muscle degeneration, vascular dysfunction, and reduced motor neuron axon outgrowth. PNAS. 2013; 110:4986–4991. doi:10.1073/pnas.1218311110. [PubMed: 23457265]
55. Selkoe DJ. Alzheimer's disease is a synaptic failure. Science. 2002; 298:789–791. doi:10.1126/science.1074069. [PubMed: 12399581]
56. Sephton CF, Good SK, Atkin S, Dewey CM, Mayer P, Herz J, Yu G. TDP-43 is a developmentally regulated protein essential for early embryonic development. J Biol Chem. 2010; 285:6826–6834. doi:10.1074/jbc.M109.061846. [PubMed: 20040602]
57. Sevigny J, Chiao P, Bussière T, Weinreb PH, Williams L, Maier M, Dunstan R, Salloway S, Chen T, Ling Y, O'Gorman J, Qian F, Arastu M, Li M, Chollate S, Brennan MS, Quintero-Monzon O, Scannevin RH, Arnold HM, Engber T, Rhodes K, Ferrero J, Hang Y, Mikulskis A, Grimm J, Hock C, Nitsch RM, Sandrock A. The antibody aducanumab reduces Aβ plaques in Alzheimer's disease. Nature. 2016; 537(7618):50–56. doi:10.1038/nature19323. [PubMed: 27582220]
58. Shankar GM, Li S, Mehta TH, Garcia-Munoz A, Shepardson NE, Smith I, Brett FM, Farrell MA, Rowan MJ, Lemere CA, Regan CM, Walsh DM, Sabatini BL, Selkoe DJ. Amyloid-beta protein dimers isolated directly from Alzheimer's brains impair synaptic plasticity and memory. Nat Med. 2008; 14:837–842. doi:10.1038/nm1782. [PubMed: 18568035]
59. Snigdha S, Smith ED, Prieto GA, Cotman CW. Caspase-3 activation as a bifurcation point between plasticity and cell death. Neurosci Bull. 2012; 28:14–24. doi:10.1007/s12264-012-1057-5. [PubMed: 22233886]
60. Stefanis L. α-Synuclein in Parkinson's disease. Cold Spring Harb Perspect Med. 2012; 2:a009399. doi:10.1101/cshperspect.a009399. [PubMed: 22355802]
61. Sze C-I, Troncoso JC, Kawas C, Mouton P, Price DL, Martin LJ. Loss of the presynaptic vesicle protein synaptophysin in hippocampus correlates with cognitive decline in Alzheimer's disease.pdf. J Neuropathol Exp Neurol. 1997; 56:933–944. [PubMed: 9258263]
62. Terry RD, Masliah E, Salmon DP, Butters N, DeTeresa R, Hill R, Hansen LA, Katzman R. Physical basis of cognitive alterations in Alzheimer's disease: synapse loss is the major correlate of cognitive impairment. Ann Neurol. 1991; 30:572–580. doi:10.1002/ana.410300410. [PubMed: 1789684]

63. Trougakos IP. The molecular chaperone apolipoprotein J/clusterin as a sensor of oxidative stress: implications in therapeutic approaches—a mini-review. Gerontology. 2013; 59:514–523. doi: 10.1159/000351207. [PubMed: 23689375]

64. Uryu K, Nakashima-Yasuda H, Forman MS, Kwong LK, Clark CM, Grossman M, Miller BL, Kretzschmar HA, Lee VM-Y, Trojanowski JQ, Neumann M. Concomitant TAR-DNA-binding protein 43 pathology is present in Alzheimer disease and corticobasal degeneration but not in other tauopathies. J Neuropathol Exp Neurol. 2008; 67:555–564. doi:10.1097/NEN.0b013e31817713b5. [PubMed: 18520774]

65. Walker AK, Spiller KJ, Ge G, Zheng A, Xu Y, Zhou M, Tripathy K, Kwong LK, Trojanowski JQ, Lee VM-Y. Functional recovery in new mouse models of ALS/FTLD after clearance of pathological cytoplasmic TDP-43. Acta Neuropathol. 2015 doi:10.1007/s00401-015-1460-x.

66. Wang W, Li L, Lin WL, Dickson DW, Petrucelli L, Zhang T, Wang X. The ALS disease-associated mutant TDP-43 impairs mitochondrial dynamics and function in motor neurons. Hum Mol Genet. 2013; 22:4706–4719. doi:10.1093/hmg/ddt319. [PubMed: 23827948]

67. Wu LS, Cheng WC, Shen CKJ. Targeted depletion of TDP-43 expression in the spinal cord motor neurons leads to the development of amyotrophic lateral sclerosis-like phenotypes in mice. J Biol Chem. 2012; 287:27335–27344. doi:10.1074/jbc.M112.359000. [PubMed: 22718760]

68. Xie H, Guan J, Borrelli LA, Xu J, Serrano-Pozo A, Bacskai BJ. Mitochondrial alterations near amyloid plaques in an Alzheimer's disease mouse model. J Neurosci. 2013; 33:17042–17051. doi: 10.1523/JNEUROSCI.1836-13.2013. [PubMed: 24155308]

69. Yang C, Wang H, Qiao T, Yang B, Aliaga L, Qiu L, Tan W, Salameh J, McKenna-Yasek DM, Smith T, Peng L, Moore MJ, Brown RH, Cai H, Xu Z. Partial loss of TDP-43 function causes phenotypes of amyotrophic lateral sclerosis. Proc Natl Acad Sci. 2014; 111:E1121–E1129. doi: 10.1073/pnas.1322641111. [PubMed: 24616503]

70. Zempel H, Thies E, Mandelkow E, Mandelkow E-M. Abeta oligomers cause localized Ca(2+) elevation, missorting of endogenous Tau into dendrites, Tau phosphorylation, and destruction of microtubules and spines. J Neurosci. 2010; 30:11938–11950. doi:10.1523/JNEUROSCI. 2357-10.2010. [PubMed: 20826658]

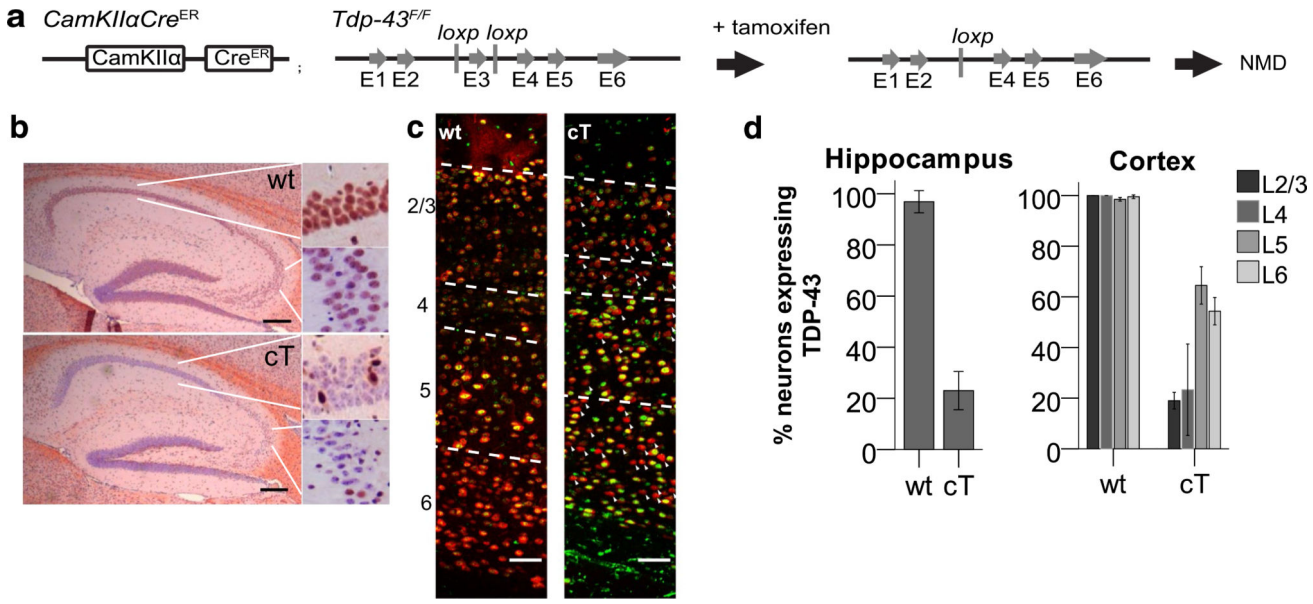

Fig. 1.

a Gene diagram of *CaMKIIα*-Cre^{ER} and *Tdp-43*$^{F/F}$ alleles. Administration of tamoxifen leads to cre-mediated excision of *Tdp-43* exon 3, and subsequent mRNA degradation through nonsense mediated decay (NMD). **b** TDP-43 N-terminal (*red*) with hematoxylin counterstain (*blue*) for representative wt and cT sections at 3 months of age in the hippocampus. **c** TDP-43 C-terminal (*green*) and NeuN (*red*) staining in the frontal cortex of representative sections from wt and cT mice. *Dashed lines* mark the boundaries of the cortical layers, *numbered on the left side. Arrowheads* indicate some neurons (NeuN, *red*) without visible TDP-43 staining. *Scale bars* **b** 200 μm, **c** 100 μm. **d** Quantifications of % neurons (NeuN+) expressing detectable TDP-43 in the hippocampus and the cortical layers of wt and cT at 3 months of age. TDP-43 is lost in 80% of pyramidal neurons in the hippocampus and cortex layers 2/3 and 4, and ~40% of pyramidal neurons in cortex layers 5 and 6 (*N*: wt = 6, cT = 5)

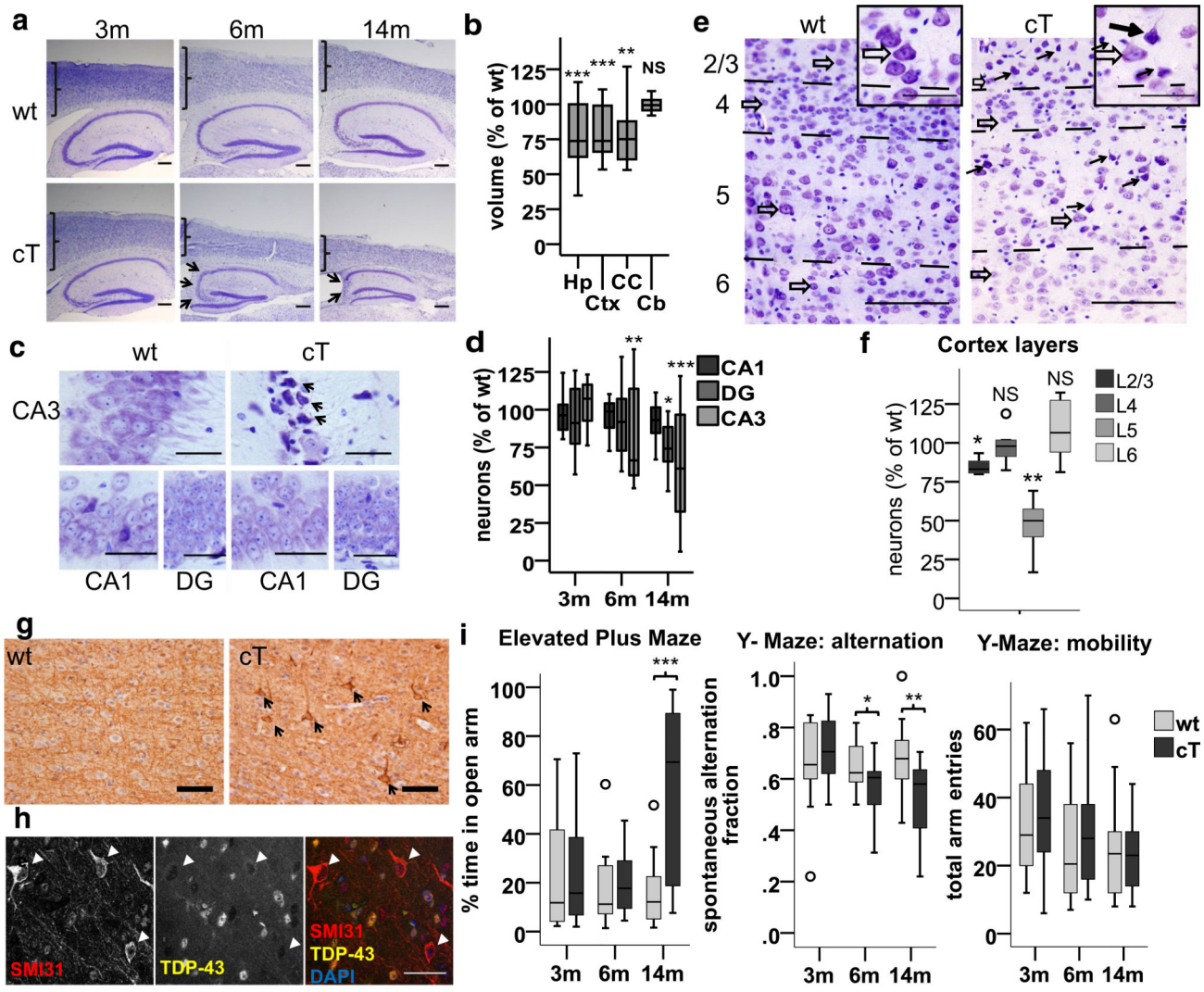

Fig. 2.

TDP-43 LOF leads to selective vulnerability in hippocampal CA3/2 and cortical Layer II/III and V neurons, and cognitive and behavioral abnormalities. **a**, **c**, **e** Representative cresyl *violet* stained slides. **a** Progressive hippocampal and cortical atrophy in cT mice, with cortical thinning and severe CA3/2 cell loss (*arrows*) at indicated ages. **b** Regional volume in cT mice is reduced in hippocampus (Hp) [$F(1,11) = 18.836$, $^{***}p = 0.001$], cortex (Ctx) [$F(1,11) = 46.435$, $^{***}p < 0.001$], and corpus callosum (CC) [Welch(1,5.505) = 19.470, $^{**}p = 0.001$], but not cerebellum (Cb) [$F(1,11) = 0.066$, $p = 0.803$], compared to wt at 8 months (n: wt = 5, ct = 8). **c** Selective degeneration of CA3/2 neurons in cT mice (some indicated by *arrows*) at 4 months, while CA1 and DG are unaffected. **d** CA3/2 neurons are selectively lost at 6 months [$t(10) = 3.428$, $^{**}p = 0.002$; wt ($M = 182.42$, SD = 54.41), cT ($M = 104.62$, SD = 11.37)], followed by the dentate gyrus (DG) at 14 months ($t(14) = 2.339$, $^{*}p = 0.035$) while CA1 neurons are unchanged [$t(14) = 1.843$, $p = 0.087$]. (3 and 6 m $n = 6$; 14 m $n = 8$). **e** CV staining in the cortical layers at 3 months of age. Degenerating neurons (*black arrows*) are numerous in layers III and V of cT mice, in contrast to normal neurons (*open arrows*). Insets show magnified healthy (*open arrows*) vs degenerating neurons (*black arrows*) in

layer V. **f** Quantification of morphologically healthy neurons revealed that neurons degenerate significantly in cortical layers 2/3 and 5, but not 4 and 6 in 3-month-old cT mice compared to wt. [Layer 2/3 $F(1,7) = 11.653$, $p = 0.011$*; Layer 4 $F(1,7) = 0.046$, $p = 0.836$ NS; Layer 5 $F(1,7) = 23.399$, $p = 0.002$**; Layer 6 $F(1,7) = 0.354$, $p = 0.570$ NS] (wt = 3, cT = 6). Outliers = ○. **g** Pathologic accumulation of phosphorylated neurofilament (SMI31, *arrows*) occurs in layer V neurons in cT mice at 3 months (*arrows*). Representative image of $N = 6$/group. **h** Co-staining of TDP-43 (*yellow*) and SMI31 (*red*) shows neurons with neurofilament pathology, which are depleted of TDP-43 (*arrowheads*) at 3 months. *Scale bars* **a** 200 μm, **c** 50 μm, **e** 100 μm. **i** Performance of cT and wt mice in the elevated plus maze and the Y-maze. *Left* cT mice show increased time in the open arm of the elevated plus maze by 14 months of age compared to wt littermates [$F(1,29) = 18.540$, $p < 0.001$]. *Middle* cT mice show significantly reduced spontaneous alternation in the Y-maze by 6 months of age compared to wt littermates [$F(1,26) = 4.536$, $p = 0.043$]. *Right* total number of arm entries in the Y-maze does not differ between cT and wt mice, even at 14 m [$F(1,29) = 0.052$, $p = 0.821$] (Outliers = ○) (3 m and 6 m $n = 14$/group; 14 m $n = 17$/group)

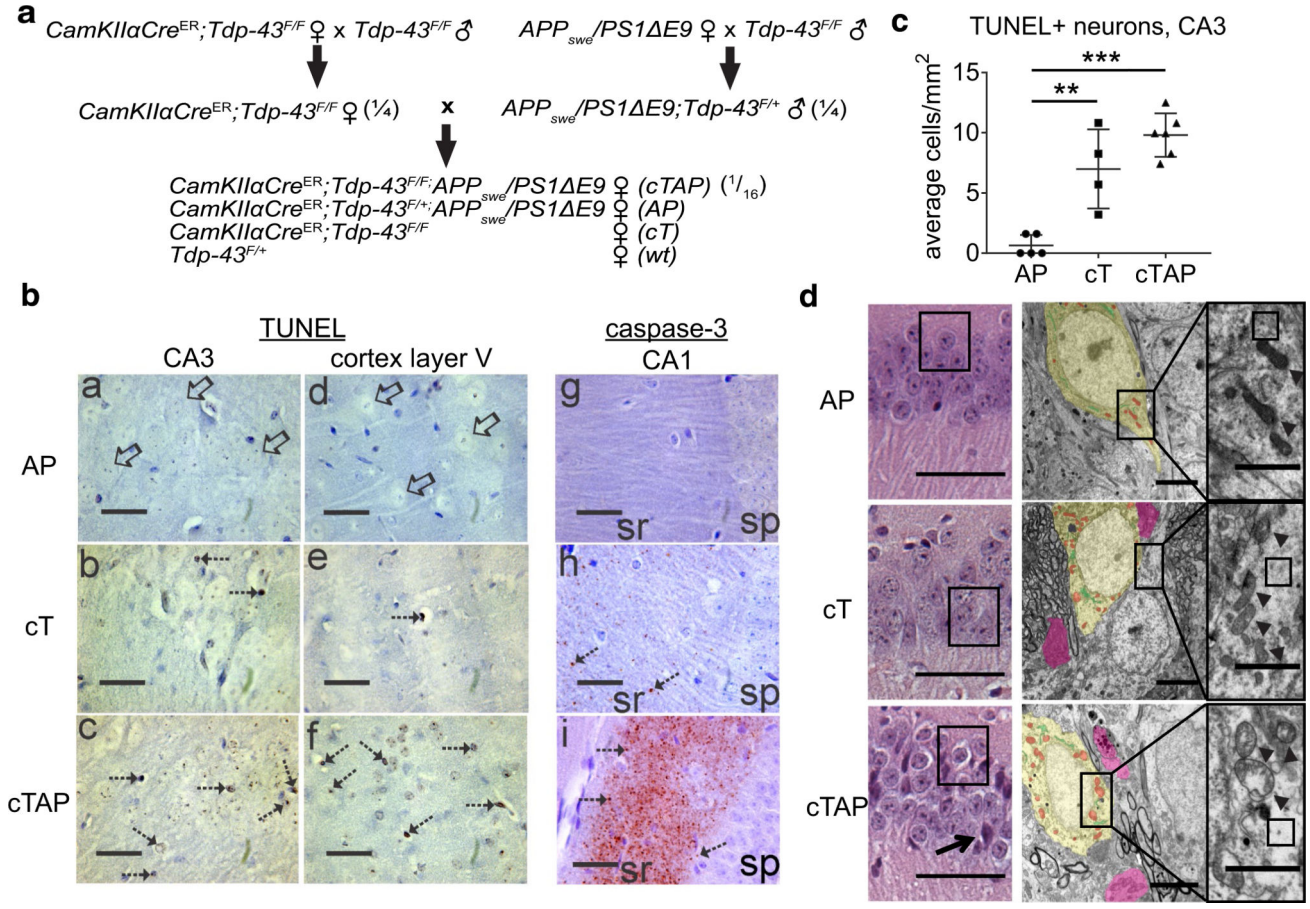

Fig. 3.

Neurodegeneration is accelerated in cTAP mice, and degenerating nuclei are TUNEL+ and caspase-3 negative, while adaptive activation of caspase-3 is observed locally at synapses of the CA1. **a** Breeding strategy for generating *CaMKIIα-Cre*^{ER};*Tdp-43*$^{F/F}$;*APP*$_{swe}$/*PS1ΔE9* mice and littermate controls. (#) Indicates the Mendelian frequency of pups from each litter expected to carry the genotype of interest. **b**: *a–f* TUNEL staining for DNA fragmentation (*hatched arrows*) is absent from AP (**b**: *a*, *d*), detectable in cT (**b**: *b*, *e*), and most prominent in cTAP mice (**b**: *c*, *f*) in degenerating regions of the hippocampus (CA3) and frontal cortex (layer V) at 3 months of age. TUNEL positive cells (*hatched arrows*) show brown nuclear labeling and attritional morphology. Neurons in the CA3 and cortex of AP mice were devoid of labeling (*open arrows*) and appeared morphologically healthy. **b**: *g–i* Cleaved caspase-3 immunoreactivity (*brown–red*) was accumulated in the striatum radiatum (sr) of CA1 but not in the stratum pyramidal layer (sp) of cTAP mice (**b**: *i*) at 8 months of age. Immunoreactivity was less conspicuous in cT mice (**b**: *h*) and was not detected in AP mice (**b**: *g*). Cleaved caspase-3 immunoreactivity appeared as punctate synaptic terminal-like staining (hatched arrows in **b**: *h*, *i*). All sections were counterstained with cresyl violet. *Scale bars* 135 μm. **c** The number of TUNEL stained neurons/mm^2 increased significantly in cT and cTAP mice compared to AP littermates [$F(1,14) = 27.23$, $p < 0.001$; Gabriel AP vs. cT $^{**}p = 0.002$, AP vs. cTAP $^{***}p < 0.001$, cT vs. cTAP NS $p = 0.131$]. **d** *Left* representative images of neurodegeneration in each genotype by H + E stain at 8 months ($N = 6$/group). Numerous

CA1 pyramidal neurons show pale staining cytoplasm in cTAP mice (*left, boxed*), in contrast to normal cytoplasm of AP and most cT neurons. Occasional darkly stained pyknotic cells (*arrow*) are also visible in cTAP mice. *Scale bars* 100 μm. *Middle and Right* electron micrographs from CA1 pyramidal neurons at 6 months show sparsely populated and discontinuous cytoplasm with loss of electron dense ribosomes (*right*, *boxed areas*) in cTAP mice, compared to cT and AP littermates. Dystrophic organelles, including mitochondria (*middle*, *red*; *right*, *arrowheads*), and Golgi/smooth ER (*middle*, *green*) are most severe in the cTAP mouse. Dystrophic neurites (*pink*) only occasionally contain lysosomes (*black*). *Scale bars* 2 μm. *N* 1/group

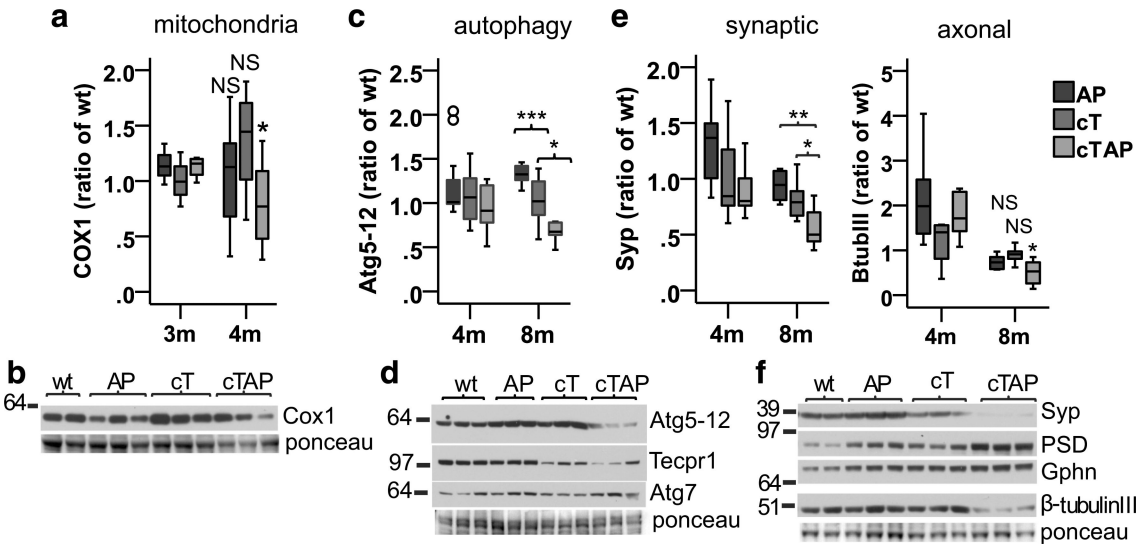

Fig. 4.

Depletion of TDP-43 accelerates loss of key neuronal proteins in the hippocampus of *APP/PS1* mice. **a** Mitochondrial Cox1 is reduced in cTAP mice [$F(3,26) = 3.044$, $p = 0.047$, Gabriel $^{*}p = 0.033$], but not AP (Gabriel $p = 0.462$) or cT (Gabriel $p = 0.397$), compared to wt littermates at 4 months. **a** Representative blot of Cox1 is shown at 4 months. **c** Atg5–12 is reduced in 8-month cTAP mice compared to AP [$F(3,20) = 11.902$, $p < 0.001$; Gabriel $^{***}p < 0.001$] and cT (Gabriel $^{*}p = 0.016$). Outliers (○). **d** Representative blots of Atg5–12, Tecpr1, and Atg7 are shown at 8 months. **e** Synaptophysin (Syp) is reduced in 8 month cTAP mice compared to AP [$F(3,20) = 8.860$, $p = 0.001$; Gabriel $^{**}p = 0.003$) and cT (Gabriel $^{*}p = 0.048$). β-Tubulin-III is reduced in 8-month cTAP mice [$F(3,20) = 5.640$, $p = 0.006$; Gabriel $^{**}p = 0.007$], but not AP (Gabriel $p = 0.290$) or cT (Gabriel $p = 0.952$) compared to wt. **f** Representative blots of synaptic and axonal markers shown at 8 months. **b–d** *N*: 4 m: wt = 9, AP = 11, cT/cTAP = 10; 8 m: wt = 5; AP = 6; cT = 7, cTAP = 6

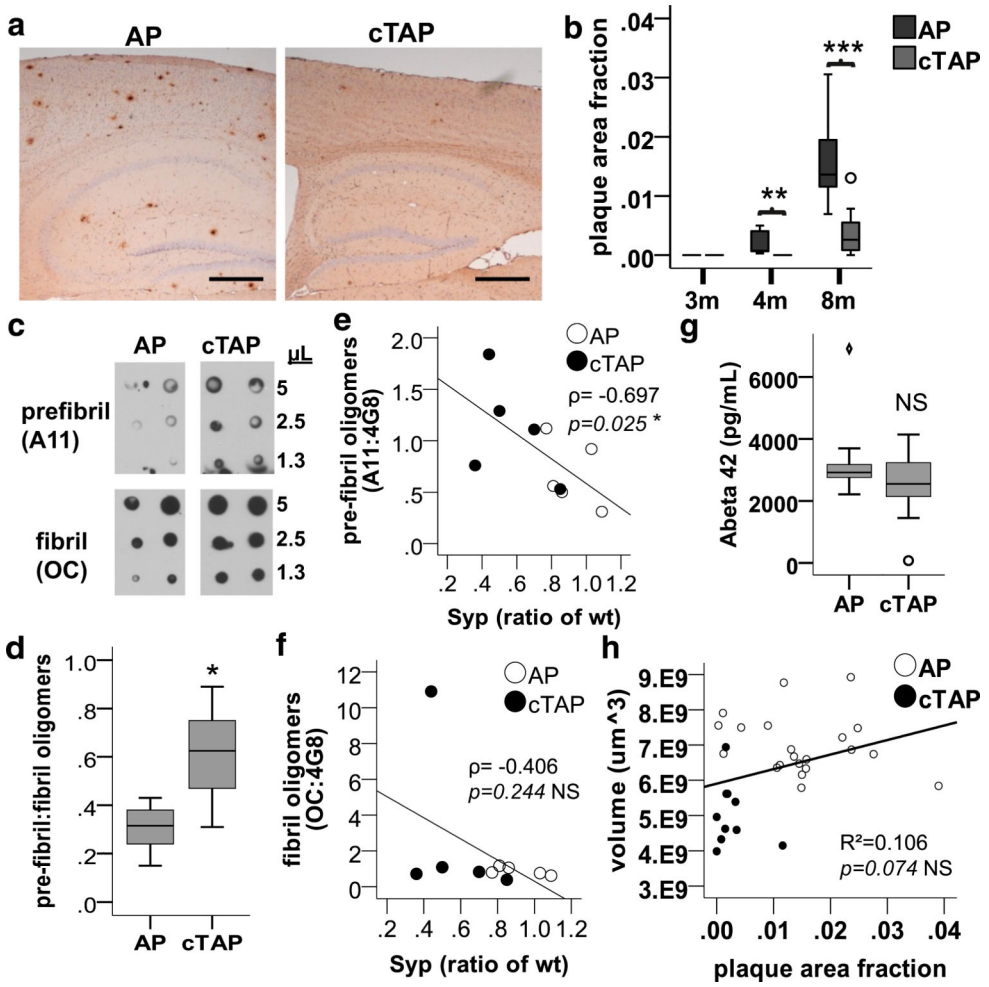

Fig. 5.

Forebrain depletion of TDP-43 increases relative levels of prefibril Aβ oligomers, while reducing Aβ plaques and fibril oligomers. **a** Representative images of 4G8 stained plaques in AP and cTAP mice at 8 months. The reduction in plaque burden in cTAP compared to AP mice is obvious by visual inspection. *Scale bars* 200 µm. **b** Plaque burden is significantly reduced in the forebrains (cortex and hippocampus) of cTAP mice compared to AP littermates at 4 months [$F(1,16) = 10.756$, $^{**}p = 0.005$] and 8 months [$F(1,18) = 30.329$, $^{***}p < 0.001$]. (3 m, 4 m $n = 9$/group; 8 m AP = 9, cTAP = 11). (Outliers = ○). **c** Representative dot blots of pre-fibril (A11) and fibril (OC) oligomers soluble in PBS after centrifuging at 100,00×*g*. **d** Relative levels of prefibril oligomers (A11:OC) were significantly increased in cTAP mice at 4 months [$F(1,10) = 6.626$, $^{*}p = 0.028$] ($n = 6$/group). **e** Pre-fibril oligomers (A11, normalized to total Aβ (4G8)) correlated inversely with synaptophysin (Syp) [Spearman's rho $\rho = -0.697$, $^{*}p = 0.025$, $n = 10$, power (1–β) = 77%] in 4-month-old mice. **f** Fibril oligomers (OC, normalized to total Aβ (4G8)) did not correlate with synaptophysin levels (Syp) [Spearman's rho $\rho = -0.406$, NS $p = 0.244$, $n = 10$] in 4-month-old mice. **g** Levels of total Aβ42 were not changed in the forebrain of cTAP mice at 4 months [Welch(1,18.987) = 2.584, $p = 0.124$] (AP = 11, cTAP = 10). (Outliers = ○, extreme cases = ◇). **h** *Scatter plot* of plaque area fraction vs. volume in the forebrain.

Linear regression analysis revealed that volume loss does not contribute significantly to plaque area fraction (R^2 = 0.106; ANOVA $F(1,29)$ = 3.425, p = 0.074; n = 31)

Table 1

Functional pathways of TDP-43-associated RNAs most likely to exert a meaningful effect on neurons

Gene	RNA fold change (TDPKO vs. ctrl)	Pathway
Cacna1b	−2.5	**Synaptic**
Dlg3	−2.7	**Synaptic**
Pitpnm3	−2.4	**Synaptic**
Ralgps2	−2.6	**Synaptic**
Vps13d	−2.4	**Synaptic**
Mrps6	−1.6	**Mitochondrial**
Tecpr1	−4	**Autophagy**
Crem	−2.5	General signaling
Brms1l	−2.1	Transcription/translation
Celf5	−2.4	Transcription/translation
Abr	−2.9	Unclear

RNAs were selected if their absolute value fold change >1.5 in TDP-43 KO brains compared to control. Pathways in bold have been strongly implicated in the early pathogenesis of AD. The RNA sequencing data were generated from 3-month cT mice [26], and the associated functional pathways in neurons were identified using GeneCards and confirmed by the manual literature search